

# Complex Kohn Variational Principle for Two-Nucleon Bound-State and Scattering with the Tensor Potential

CARLOS F. DE ARAUJO, JR., SADHAN K. ADHIKARI, AND LAURO TOMIO

*Instituto de Física Teórica, Universidade Estadual Paulista, 01405-000 São Paulo, São Paulo, Brazil*

Received September 17, 1993; revised September 9, 1994

Complex Kohn variational principle is applied to the numerical solution of the fully off-shell Lippmann–Schwinger equation for nucleon–nucleon scattering for various partial waves including the coupled  ${}^3S_1$ – ${}^3D_1$  channel. Analytic expressions are obtained for all the integrals in the method for a suitable choice of expansion functions. Calculations with the partial waves  ${}^1S_0$ ,  ${}^1P_1$ ,  ${}^1D_2$ , and  ${}^3S_1$ – ${}^3D_1$  of the Reid soft core potential show that the method converges faster than other solution schemes not only for the phase shift but also for the off-shell  $t$  matrix elements. We also show that it is trivial to modify this variational principle in order to make it suitable for bound-state calculation. The bound-state approach is illustrated for the  ${}^3S_1$ – ${}^3D_1$  channel of the Reid soft-core potential for calculating the deuteron binding, wave function, and the  $D$  state asymptotic parameters. © 1995 Academic Press, Inc.

## I. INTRODUCTION

Variational principles (v.p.'s) have frequently been successfully applied to the solution of quantum scattering problems [1–8]. Most of the commonly used v.p.'s are either of the Schwinger [1] or of the Kohn [2] type. There are also less frequently used higher order v.p.'s [4]. The Schwinger type v.p.'s are usually applied to the solution of the momentum space Lippmann–Schwinger equation [9] which generate the off-shell  $t$  matrix elements in addition to the phase shifts, whereas the Kohn type v.p.'s are usually applied to the calculation of the phase shifts via the configuration space Schrödinger equation.

The usual Kohn v.p., unlike the Schwinger and the higher order v.p.'s, does not require the calculation of integrals involving the free Green function and numerically is the simplest of all available v.p.'s. The Kohn v.p. for the on-shell  $K$  matrix elements requires trial functions satisfying scattering boundary conditions. It was noted by Schwartz [10] that the  $K$  matrix calculated by the Kohn v.p. occasionally exhibits anomalous singularities in the scattering region. This fact has limited significantly the use of the Kohn v.p.. The Schwinger v.p. [1], on the other hand, requires the tedious evaluation of integrals involving the free Green function. The advantage of the Kohn v.p. over the Schwinger v.p. in having simple integrals to deal

with is more than offset by the presence of anomalous singularities in the Kohn v.p. [10].

As an attempt to maintain the above advantages of the Kohn method and reduce the troubles associated with the anomalous singularities, it has recently been suggested that by choosing the complex boundary conditions for the Green function the Kohn v.p. readily yields the complex  $t$  matrix elements [11, 12]. It was first claimed that this so-called complex Kohn v.p. does not present anomalous singularities. [11] However, later it has been demonstrated in two different studies [13] that in the complex Kohn v.p. the anomalous singularities could appear. However, these singularities are extremely rare. It should be noted that the Schwinger variational method itself can also have anomalous singularities in cases where the complex Kohn method is free of them [14]. Also, it has been demonstrated that the complex Kohn v.p. may lead to a rapid convergence, compared to Schwinger and other type v.p.'s for different problems in atomic physics [11, 12].

We show how the ideas behind the complex Kohn v.p. could be modified to lead to an efficient method for the bound state problem (including the coupled angular momentum states) for calculating the binding energy, bound state wave functions, and the asymptotic normalization parameters for the bound state wave function.

The complex Kohn v.p. has seen extensive application to molecular problems, including both electron–molecule scattering and chemically reactive molecular collisions [15]. In both of these applications the problems are inherently many channeled including many partial waves and several electronic states in the case of electron–molecule scattering and including many target rotational–vibrational states in the case of reactive molecular collisions. In the present work we test the complex Kohn v.p. for nucleon–nucleon scattering with “realistic” Reid potentials [16] in various angular momentum states possessing a soft core, where precision calculations have been performed with other methods [4, 5, 8, 16, 17]. This will allow us to compare the results of the complex Kohn v.p. with other methods. Accurate numerical solutions of this problem are of interest to a variety of research problems, such as, the two- and the

three-nucleon bound-state and scattering studies, including their photo- and electro-desintegration.

Here we develop the necessary modifications of the complex Kohn v.p. to include coupling between different angular momentum states in the presence of the tensor force of the nucleon–nucleon system. The present generalization not only allows us to calculate the phase-shifts and mixing parameters in the coupled  ${}^3S_1$ – ${}^3D_1$  channel, but also the momentum-space off-shell  $t$  matrix elements. Usually, the Kohn v.p. is used for calculating the phase shifts in the configuration space in the absence of angular momentum coupling. This is the first application of the complex Kohn v.p. to the calculation of phase shifts, off-shell  $t$  matrix elements, and the bound-state observables for coupled angular momentum states. We study here the  ${}^1S_0$ ,  ${}^1P_1$ ,  ${}^1D_2$ , and  ${}^3S_1$ – ${}^3D_1$  channels of nucleon–nucleon scattering using the Reid soft-core potentials [16].

For the  ${}^3S_1$ – ${}^3D_1$  channel we used the Peiper’s modification [17] of the Reid potential. This potential has simple analytic forms and, hence, the integrals of this method are evaluated analytically. So the only numerical task is the inversion of a relatively small matrix and matrix vector multiplication. We are using this potential [16] for its simplicity; otherwise the numerical difficulties encountered (with the soft core) in this potential are the same as in other meson theoretic potentials. We found excellent convergence in all the partial waves studied, including the coupled  ${}^3S_1$ – ${}^3D_1$  state. This should motivate the use of this method to the solution of the nucleon–nucleon scattering and bound-state problems with other realistic potentials and to the solution of other realistic few-nucleon scattering problems. However, in other realistic situations one may have to evaluate the integrals of the method numerically.

Because of the presence of the soft core, these realistic potentials are difficult to deal with both in configuration and momentum spaces. There are difficulties with the configuration space integration for small  $r$ . In a momentum space treatment the momentum space infinite integrals are discretized for employing a momentum space mesh which extends to a very large value of momentum, which is difficult to deal with numerically. This problem is extremely acute in the physically interesting  ${}^3S_1$ – ${}^3D_1$  channel in the presence of the soft core. Hence the study of the nucleon–nucleon scattering and bound-state problems with Reid soft-core potentials in this channel should provide a stringent test for the applicability of the complex Kohn v.p. to other problems of nuclear physics.

We find that for these partial waves of the nucleon–nucleon system, the complex Kohn v.p. produces excellent convergence for the phase shifts, the mixing parameters of the coupled angular momentum states, the off-shell  $t$  matrix elements, and binding energy and bound-state wave functions. The possibility of the accidental appearance of anomalous singularities seems to have no relevance to the usefulness of this method. In this problem, the final convergence is far better than that obtained with the Schwinger v.p.

The plan of the paper is as follows. In Section II we present

the complex Kohn v.p. for the scattering problem and show how it could be applied to the bound-state problem. In Section III we present the explicit momentum space matrix elements and their analytic results for the Yukawa potential. In Section IV we present the numerical results for the nucleon–nucleon bound-state and scattering problems. Finally, in Section V we present a brief summary.

## II. COMPLEX KOHN VARIATIONAL PRINCIPLE

The Lippmann–Schwinger [9] equation is written in the operator form

$$t(E) = V + VG_0^{(+)}(E)t(E), \quad (2.1)$$

where  $t$  is the transition matrix,  $V$  is the potential, and  $G_0^{(+)}(E) \equiv (E - H_0 + i0)^{-1}$  is the free Green function at the center of mass (c.m.) energy  $E$ , with  $H_0$  the free Hamiltonian.

The explicit momentum-space partial-wave Lippmann–Schwinger equation for central potentials is given by

$$t_L(p', p, E) = v_L(p', p) + \frac{2}{\pi} \int_0^\infty q^2 dq \frac{v_L(p', q)t_L(q, p, E)}{k^2 - q^2 + i0}, \quad (2.2)$$

where  $m$  is the reduced mass,  $v \equiv 2mV/\hbar^2$ ,  $L$  is the angular momentum label, and  $k^2 \equiv 2mE/\hbar^2$  with  $k$  the on-shell momentum. For coupled angular momentum channels the generalization of the above partial-wave Lippmann–Schwinger equation is

$$t_{LL}(p', p, E) = v_{LL}(p', p) + \frac{2}{\pi} \sum_{L'} \int_0^\infty q^2 dq \frac{v_{LL}(p', q)t_{LL}(q, p, E)}{k^2 - q^2 + i0}. \quad (2.3)$$

For the nucleon–nucleon problem one has an equation of type (2.3) in the presence of tensor potential for the coupled angular momentum states  ${}^3S_1$ – ${}^3D_1$ . With this definition, the phase-shift  $\delta_L$  in the uncoupled channel is defined by

$$t_L(k, k, E) = -\frac{e^{i\delta_L} \sin \delta_L}{k}. \quad (2.4)$$

The on-shell  $S$  matrix is defined in terms of the fully on-shell  $t$  matrix by

$$S_{LL}(k, k; E) = \delta_{LL} - 2ikt_{LL}(k, k, E). \quad (2.5)$$

In the coupled  ${}^3S_1$ – ${}^3D_1$  channel we use the Stapp parametrization [18] of the  $S$  matrix to define the nuclear bar phase-shifts ( $\delta_L$ ) and mixing parameters ( $\epsilon_1$ ). The Stapp parametrization is defined by

$$S = \begin{pmatrix} \cos 2\varepsilon_1 e^{2i\delta_{j-1}} & i \sin 2\varepsilon_1 e^{i(\delta_{j-1} + \delta_{j-1})} \\ i \sin 2\varepsilon_1 e^{i(\delta_{j-1} + \delta_{j-1})} & \cos 2\varepsilon_1 e^{2i\delta_{j+1}} \end{pmatrix} \quad (2.6)$$

Here  $J$  is the total angular momentum, so that the orbital angular momenta are  $(J \pm 1)$ . It is to be noted that there is also another parametrization of the  $S$  matrix due to Blatt and Biedenharn [19].

The complex Kohn v.p. for the on-shell  $t$  or  $S$  matrix elements for uncoupled channels could easily be extended to include angular momentum coupled channels and off-shell  $t$  matrix elements. This is conveniently done by considering the complex Kohn v.p. as the degenerate kernel solution of Eq. (2.1) with the degenerate approximation to the free Green function  $G_0^{(+)}(E)$  [11],

$$[G_0^{(+)}(E)]_N = \sum_{n,j=1}^N |u_n\rangle D_{nj} \langle u_j|, \quad (2.7)$$

where

$$(D^{-1})_{jn} = \langle u_j | (E - H_0) | u_n \rangle, \quad (2.8)$$

where  $u_j$ ,  $j = 1, 2, \dots, N$ , is a set of arbitrary chosen functions. For numerical calculation, Eq. (2.7) is to be interpreted as one in the partial wave form. These functions should satisfy the small and large  $r$  behavior of the partial-wave configuration space free Green function in order that the approximation given by Eq. (2.7) is a good one. The configuration space matrix elements of Eq. (2.7) for angular momentum  $L$  should satisfy the asymptotic behavior of the partial-wave free Green function:

$$G_{0(L)}^{(+)}(r, r', E) = ik j_L(kr_<) h_L^{(+)}(kr_>), \quad (2.9)$$

where  $j_L$  and  $h_L^{(+)}$  are the usual spherical Bessel and Hankel functions, and  $r_>$  ( $r_<$ ) is the larger (smaller) of  $r$  and  $r'$ . Equation (2.9) is symmetric in  $r$  and  $r'$  and satisfies the following conditions for small and large  $r$  for a fixed  $r'$ :

$$\lim_{r \rightarrow \infty} G_{0(L)}^{(+)}(r, r', E) = \frac{e^{ikr}}{r} \times \text{function}(r'), \quad E = \hbar^2 k^2 / (2m) > 0, \quad (2.10)$$

$$\lim_{r \rightarrow \infty} G_{0(L)}^{(+)}(r, r', E) = \frac{e^{-\beta r}}{r} \times \text{function}(r'), \quad E = \hbar^2 \beta^2 / (2m) < 0, \quad (2.11)$$

$$\lim_{r \rightarrow 0} G_{0(L)}^{(+)}(r, r', E) = r^L \times \text{function}(r'). \quad (2.12)$$

In the bound-state problem  $\hbar^2 \beta^2 / (2m)$  is the binding energy. A similar set of equations exist for the roles of  $r$  and  $r'$  interchanged in Eqs. (2.10)–(2.12).

The approximate degenerate Green function of Eq. (2.7) can be easily made to satisfy the boundary conditions (2.10)–(2.12),

provided that the function  $u_i(r) \equiv \langle u_i | r \rangle \equiv \langle r | u_i \rangle$  is taken to satisfy [11]

$$\lim_{r \rightarrow \infty} u_{1(L)}(r) \rightarrow \frac{e^{ikr}}{r} \quad (2.13)$$

for scattering, and

$$\lim_{r \rightarrow \infty} u_{1(L)}(r) \rightarrow \frac{e^{-\beta r}}{r} \quad (2.14)$$

for bound states, as well as

$$\lim_{r \rightarrow 0} u_{1(L)}(r) \rightarrow r^L \quad (2.15)$$

for both scattering and bound states.

The remaining functions  $u_j(r) \equiv \langle u_j | r \rangle \equiv \langle r | u_j \rangle$ ,  $j > 1$ , are taken to satisfy

$$\lim_{r \rightarrow \infty} u_{j(L)}(r) \rightarrow 0, \quad (2.16)$$

$$\lim_{r \rightarrow 0} u_{j(L)}(r) \rightarrow r^L. \quad (2.17)$$

It is to be noted that in order to satisfy the boundary conditions for scattering,  $\langle u_j | r \rangle$  and  $\langle r | u_j \rangle$  are taken to be equal and not complex conjugates of each other. We consider the following simple set of functions satisfying these conditions:

$$u_{1(L)}(r) = \frac{e^{ikr}}{r} (1 - e^{-\alpha r})^{L+1} \quad (2.18)$$

for scattering and

$$u_{j(L)}(r) = \frac{e^{-\beta r}}{r} (1 - e^{-\alpha r})^{L+1} \quad (2.19)$$

for bound state, and

$$u_{j(L)}(r) = r^L e^{-(j-1)\alpha r}, \quad j = 2, 3, \dots, N, \quad (2.20)$$

for both scattering and bound state. Here the variational parameter  $\alpha$  is to be adjusted numerically to obtain the best convergence. It is obvious that this is not the only possible choice for the functions  $u_j$ ; there could be many other choices. The objective of this work is not to exhaust all possibilities, but to see if this simple choice provides good convergence for the nucleon–nucleon scattering and bound-state problems involving tensor potential and a soft core.

When degenerate (separable) approximation (2.7) is used in the Lippmann–Schwinger equation (2.1), it yields the solution [11]

$$t_N(E) = V + \sum_{n,j=1}^N V|u_n\rangle J_{nj}\langle u_j|V, \quad (2.21)$$

where

$$(J^{-1})_{jn} = \langle u_j|(E - H_0 - V)|u_n\rangle. \quad (2.22)$$

This is the desired complex Kohn v.p. for the  $t$  matrix. The variational property of the on-shell version of Eq. (2.21) has been established before [11]. The same variational property also holds for the off-shell version of this equation. As in the usual real Kohn v.p. in order to evaluate the  $t$  matrix via Eqs. (2.21) and (2.22) one does not require integrals involving the Green function.

Equations (2.21) and (2.22) are suitable for scattering calculation. For bound-state calculation it is more convenient to consider only the full Green function  $G(E) = (E - H)^{-1}$  with the degenerate approximation (2.7) for the free Green function. This yields in coordinate space the approximation

$$G_N(r, r'; E) = \sum_{n,j=1}^N \langle r|u_n\rangle J_{nj}\langle u_j|r'\rangle, \quad (2.23)$$

with  $J_{nj}$  given by Eq. (2.22). At the bound-state energy, the matrix  $J^{-1}$  has determinant zero. This condition of zero determinant determines the binding energy. This bound-state condition which results from the Kohn method is the standard Rayleigh–Ritz variational method [3]. However, in order to determine the bound-state wave function in the Rayleigh–Ritz method one has to solve an eigenfunction–eigenvalue problem. In the present case the bound-state wave function,  $\psi_L(r)$ , is obtained from the residue of the Green function,  $G(E)$ , at the bound-state pole, which has the following behavior:

$$\lim_{k \rightarrow i\beta} G_L(r, r'; E) = \frac{\psi_L(r)\psi_L(r')}{E + \hbar^2\beta^2/(2m)}. \quad (2.24)$$

For large  $N$ ,  $G_N(E)$  of Eq. (2.23) is expected to satisfy the limiting behavior (2.24). Hence, the residue of  $G_N(r, r', E)$  of Eq. (2.23) at the bound-state pole for large  $N$  yields the bound-state wave function. We shall use this simple modification of the complex Kohn method for the calculation of the deuteron binding energy, bound-state wave function, and asymptotic parameters for the wave function.

### III. EXPLICIT MATRIX ELEMENTS

One reason for choosing the expansion functions (2.18)–(2.20) is that for the commonly used Yukawa and exponential potentials all the matrix elements needed in the numerical evaluation of the  $t$  matrix elements can then be evaluated analytically. The Reid potentials that we shall use are expressed in terms of linear combinations of Yukawa potentials. Consequently,

with the expansion functions (2.18)–(2.20) the only numerical task is the evaluation of an analytically known matrix and simple matrix vector multiplication.

The explicit matrix elements of the  $t$  matrix (2.21) is given by

$$t_{L'L}(p', p, E) = v_{L'L}(p', p) + \sum_{nL',jL''} \langle p'L'|v_{L'L'}|u_{nL'}\rangle J_{nL',jL''}\langle u_{jL''}|v_{L'L}|pL\rangle, \quad (3.1)$$

with

$$(J^{-1})_{jL'',nL'} = \left\langle u_{jL''} \left[ \left( k^2 + \frac{d^2}{dr^2} - \frac{L(L+1)}{r^2} \right) \delta_{L'',L'} - v_{L''L'} \right] \right| u_{nL'} \rangle. \quad (3.2)$$

In the case of a central potential  $v_{L'L}(p', p) = \delta_{L'L}v_L(p', p)$  and Eq. (3.1) simplifies to its diagonal form:

$$t_L(p', p, E) = v_L(p', p) + \sum_{nL,jL} \langle p'L|v_L|u_{nL}\rangle J_{nL,jL}\langle u_{jL}|v_L|pL\rangle. \quad (3.3)$$

The potential  $v$  used in the present calculation has the general form

$$v(r) = v_c(r) + v_T(r)S_{12} + v_{LS}(r)L \cdot S, \quad (3.4)$$

with

$$S_{12} = 3 \frac{(\boldsymbol{\sigma}_1 \cdot \mathbf{r})(\boldsymbol{\sigma}_2 \cdot \mathbf{r})}{r^2} - (\boldsymbol{\sigma}_1 \cdot \boldsymbol{\sigma}_2), \quad (3.5)$$

where  $\boldsymbol{\sigma}_1, \boldsymbol{\sigma}_2$ , are usual Pauli spin operators for the two particles. The form (3.4) is applicable for the  ${}^3S_1$ – ${}^3D_1$  channel in the presence of the tensor ( $v_T(r)$ ) and spin-orbit ( $v_{LS}(r)$ ) interactions. In the  ${}^3S_1$ – ${}^3D_1$  channel  $v_{00} = v_c$ ,  $v_{02} = v_{20} = \sqrt{8}v_T$ , and  $v_{22} = v_c - 2v_T - 3v_{LS}$ . In the case of other potentials considered here, however, one has  $v_T(r) = v_{LS}(r) = 0$ .

The  ${}^3S_1$ – ${}^3D_1$  potential used in this study is Pieper's simplification [17] of the Reid soft-core (RSC) potential, referred to as the simplified Reid soft-core (SRSC) potential. Pieper writes the Reid soft-core potential for this channel as a linear combination of Yukawa potentials which can be easily handled numerically. Otherwise, numerically, the RSC potential is indistinguishable from the SRSC potential, and so are the two-nucleon observables of these two potentials.

For the sake of completeness we provide here the potentials used in this study. Explicitly, all the potentials have the form

$$V(r) = \sum_{j=1}^M V_j r^{-1} e^{-\mu_j r}. \quad (3.6)$$

For the  ${}^1S_0$  RSC potential  $M = 3$  and  $V_1 = -10.463/0.7$  MeV fm,  $V_2 = -1650.6/0.7$  MeV fm,  $V_3 = 6484.2/0.7$  MeV fm,  $\mu_1 = 0.7$  fm $^{-1}$ ,  $\mu_2 = 4\mu_1$ , and  $\mu_3 = 7\mu_1$ .

For the  ${}^3S_1$ - ${}^3D_1$  SRSC potential  $M = 4$  for each of  $V_C$ ,  $V_T$ , and  $V_{LS}$ . For  $V_C$ ,  $V_1 = -10.463/0.7$  MeV fm,  $V_2 = 105.468/0.7$  MeV fm,  $V_3 = -3187.8/0.7$  MeV fm, and  $V_4 = 9924.3/0.7$  MeV fm; for  $V_T$ ,  $V_1 = -18.5488/0.7$  MeV fm,  $V_2 = -109.307/0.7$  MeV fm,  $V_3 = 210.503/0.7$  MeV fm,  $V_4 = -1650.35/0.7$  MeV fm; and for  $V_{LS}$ ,  $V_1 = V_2 = 0$ ,  $V_3 = 708.91/0.7$  MeV fm,  $V_4 = -2713.1/0.7$  MeV fm. In all cases  $\mu_1 = 0.7$  fm $^{-1}$ ,  $\mu_2 = 2\mu_1$ ,  $\mu_3 = 4\mu_1$ , and  $\mu_4 = 6\mu_1$ .

For the  ${}^1P_1$  RSC potential  $M = 3$ ,  $V_1 = 31.399/0.7$  MeV fm,  $V_2 = -634.39/0.7$  MeV fm,  $V_3 = 2163.4/0.7$  MeV fm,  $\mu_1 = 0.7$  fm $^{-1}$ ,  $\mu_2 = 2\mu_1$ ,  $\mu_3 = 3\mu_1$ .

For the  ${}^1D_2$  RSC potential  $M = 4$  and  $V_1 = -10.463/0.7$  MeV fm,  $V_2 = -12.322/0.7$  MeV fm,  $V_3 = -1112.6/0.7$  MeV fm,  $V_4 = 6484.2/0.7$  MeV fm,  $\mu_1 = 0.7$  fm $^{-1}$ ,  $\mu_2 = 2\mu_1$ ,  $\mu_3 = 4\mu_1$ , and  $\mu_4 = 7\mu_1$ .

The matrix elements of Eqs. (3.1)–(3.2) are explicitly written as

$$(J^{-1})_{jL'nL'} = \int_0^\infty [ru_{jL'}] \left[ \left( k^2 + \frac{d^2}{dr^2} - \frac{L(L+1)}{r^2} \right) \right. \quad (3.7)$$

$$\left. \delta_{L'nL'} - v_{L'nL'}(r) \right] [ru_{nL'}] dr,$$

$$\langle pL|V_{LL'}|u_{nL'}\rangle \equiv \langle u_{nL'}|V_{L'L}|pL\rangle = \int_0^\infty u_{nL'}(r)v_{LL'}(r)j_L(pr)r^2 dr, \quad (3.8)$$

$$V_{LL'}(p, q) \equiv V_{L'L}(q, p) = \int_0^\infty j_L(pr)V(r)j_{L'}(qr)r^2 dr. \quad (3.9)$$

Next we provide the explicit momentum space matrix elements for the following Yukawa potential

$$v(r) = v_0 \frac{e^{-\mu r}}{r}. \quad (3.10)$$

In this case

$$v_{LL}(p, q) = \frac{v_0}{2pq} Q_L \left[ \frac{\mu^2 + p^2 + q^2}{2pq} \right], \quad (3.11)$$

$$v_{20}(p, q) \equiv v_{02}(q, p) = -\frac{v_0}{2pq} \left[ Q_2 \left( \frac{q + i\mu}{p} \right) + Q_2 \left( \frac{q - i\mu}{p} \right) \right], \quad (3.12)$$

$$\begin{aligned} \left\langle u_{1L} \left[ \left[ \left( k^2 + \frac{d^2}{dr^2} - \frac{L(L+1)}{r^2} \right) \delta_{LL'} - v_{LL'} \right] \right] u_{1L'} \right\rangle &= \delta_{LL'} \left[ -\alpha^2(L+1)^2 \sum_{j=0}^{2L} \frac{(-1)^j C_j^{2L}}{(2+j)\alpha - 2ik} \right. \\ &\quad \left. - L(L+1) \sum_{j=0}^{2L+2} (-1)^j C_j^{2L+2} [j\alpha - 2ik] \ln[j\alpha - 2ik] \right] \\ &\quad + v_0 \sum_{j=0}^{L+L'+2} (-1)^j C_j^{L+L'+2} \ln(\mu + j\alpha - 2ik), \end{aligned} \quad (3.13)$$

$$\begin{aligned} \left\langle u_{nL} \left[ \left[ \left( k^2 + \frac{d^2}{dr^2} - \frac{L(L+1)}{r^2} \right) \delta_{LL'} - v_{LL'} \right] \right] u_{1L'} \right\rangle &= \left\langle u_{1L'} \left[ \left[ \left( k^2 + \frac{d^2}{dr^2} - \frac{L(L+1)}{r^2} \right) \delta_{L'L} - v_{L'L} \right] \right] u_{nL} \right\rangle \\ &= -\delta_{L'L}(L+1)! \sum_{j=0}^{L+1} (-1)^j C_j^{L+1} \frac{((n-1)\alpha)^2 + 2\alpha(n-1)(\alpha j - ik) - k^2}{[\alpha(n+j-1) - ik]^{L+2}} \\ &\quad - L!v_0 \sum_{j=0}^{L'+1} (-1)^j C_j^{L'+1} [\mu + \alpha(n+j-1) - ik]^{-(L'+1)}, \end{aligned} \quad (3.14)$$

$$\begin{aligned} \left\langle u_{nL} \left[ \left[ \left( k^2 + \frac{d^2}{dr^2} - \frac{L(L+1)}{r^2} \right) \delta_{L'L} - v_{L'L} \right] \right] u_{mL'} \right\rangle &= (L+L'+1)! \left[ \frac{2(k^2 - (n-1)(m-1)\alpha^2)(L+1)}{[\alpha(m+n-2)]^{2L+3}} \delta_{L'L} \right. \\ &\quad \left. - v_0 \frac{1}{[\alpha(n+m-2) + \mu]^{L+L'+2}} \right], \end{aligned} \quad (3.15)$$

$$\langle pL|v_{LL}|u_{nL}\rangle = v_0 \frac{p^L(\sqrt{2})^{L(L+1)}}{[p^2 + \{\mu + \alpha(n-1)\}]^{L+1}}, \quad (3.16)$$

$$\langle p0|v_{02}|u_{n2}\rangle = 2v_0 \frac{3[\alpha(n-1) + \mu]^2 - p^2}{[p^2 + \{\mu + \alpha(n-1)\}^2]^3}, \quad (3.17)$$

$$\langle p2|v_{20}|u_{n0}\rangle = \frac{v_0}{p^2} \left[ \frac{2p^2 + 3[\mu + \alpha(n-1)]^2}{p^2 + [\mu + \alpha(n-1)]^2} - \frac{3[\mu + \alpha(n-1)]}{p} \arctan \left( \frac{p}{\mu + \alpha(n-1)} \right) \right], \quad (3.18)$$

$$\langle pL|v_{LL}|u_{L'}\rangle = \frac{i^{L+1}v_0}{p} \sum_{j=0}^{L'+1} (-1)^j C_j^{L'+1} Q_L \left[ \frac{k + i(\mu + \alpha j)}{p} \right]. \quad (3.19)$$

In these equations  $C_j^M = M!/j!(M-j)!$ ,  $Q_L$  is the usual Legendre function of second kind. The above equations are valid for scattering calculation for  $L, L' = 0, 1, 2$ . For bound-state calculation one should change  $k \rightarrow i\beta$  in these equations.

#### IV. NUMERICAL RESULTS

In order to see how the complex Kohn v.p. works in practice, we performed numerical calculations with the semiphenomenological  ${}^1S_0$ ,  ${}^1P_1$ , and  ${}^1D_2$  RSC and  ${}^3S_1$ - ${}^3D_1$  SRSC potentials defined in the last section. These potentials have the realistic soft core and one pion exchange tail numerically built in. These potentials are used in actual few-nucleon calculations and their numerical treatment is known to lead to all complications of a realistic meson-theoretic potential. So if we can demonstrate good convergence with these potentials, especially in the  ${}^3S_1$ - ${}^3D_1$  channel, one could be assured of good convergence in other cases.

The parameter  $\alpha$  in the expansion functions is supposed to be varied in order to improve the convergence. The convergence was good for a wide range of values of  $\alpha$ . Although a specific value of  $\alpha$  leads to an excellent convergence for a specific case—energy and potential—we decided to choose one particular  $\alpha$  for all possible energies and potentials. The value finally chosen after some experimentation is  $\alpha = 1.15 \text{ fm}^{-1}$  both for scattering and bound-state studies in all partial waves. We also employ  $\hbar^2/(2m) = 41.47 \text{ MeV fm}^2$ .

The approximate  $t$  matrices of Eqs. (3.1) and (3.2) do not, however, satisfy the constraints of unitarity. Hence, the  $S$  matrix constructed with them via Eqs. (2.5) and (2.6) is not unitary and the phase-shifts are complex. The real part of these phase shifts defined by

$$\delta_r = \frac{1}{2} \arctan \frac{\text{Im}(S)}{\text{Re}(S)}, \quad (4.1)$$

will be considered as the phase-shift of the variational  $t$  matrix. The violation of unitarity is small for large  $N$  and is insignificant in the converged result.

In Table I we present the elastic scattering phase-shifts  $\delta_L$  and the mixing parameter  $\varepsilon_1$  at various energies for different

values of  $N$ . The calculation with a specific value  $N$  of  $N$  for the uncoupled channel means that the first  $N$  functions of the set (2.18)–(2.20) has been used. This leads to a matrix  $J$  of dimension  $N$ . For the coupled  ${}^3S_1$ - ${}^3D_1$  channel it means that the first  $N$  functions of the set (2.18)–(2.20) have been used for both  $L = 0$  and  $L = 2$ . Consequently, this leads to a matrix  $J$  of dimension  $2N$ .

From Table I we see that the phase-shifts converge rapidly in all cases including the coupled  ${}^3S_1$ - ${}^3D_1$  channel. In order to check the possible existence of any hidden systematic errors in all these situations, we also compared the results with the phase-shifts calculated by completely different methods, such

TABLE I

Phase Shifts for the  ${}^1S_0$ ,  ${}^1P_1$ ,  ${}^1D_2$ , and  ${}^3S_1$ - ${}^3D_1$  Reid Soft-Core Potentials for Different  $N$  and at Different Energies

$E_{cm}$	Potential	$N = 2$	$N = 4$	$N = 6$	$N = 8$	$N = 10$
12	${}^1S$ ( $\delta_0$ )	0.3244	0.7665	0.8557	0.8604	0.8606
	${}^1P$ ( $\delta_1$ )	0.0140	-0.0294	-0.0330	-0.0332	-0.0332
	${}^1D$ ( $\delta_2$ )	0.0094	0.0112	0.0113	0.0113	0.0113
	${}^3S$ - ${}^3D$ ( $\delta_0$ )	0.8131	1.3450	1.4217	1.4262	1.4262
	${}^3S$ - ${}^3D$ ( $\delta_2$ )	-0.0686	-0.0510	-0.0504	-0.0501	-0.0501
	${}^3S$ - ${}^3D$ ( $\varepsilon_1$ )	0.1192	0.0403	0.0328	0.0318	0.0318
48	${}^1S$ ( $\delta_0$ )	-0.4385	0.3241	0.4341	0.4400	0.4402
	${}^1P$ ( $\delta_1$ )	-0.1241	-0.1878	-0.1899	-0.1896	-0.1896
	${}^1D$ ( $\delta_2$ )	0.0691	0.0633	0.0610	0.0602	0.0599
	${}^3S$ - ${}^3D$ ( $\delta_0$ )	0.4347	0.6990	0.7438	0.7485	0.7485
	${}^3S$ - ${}^3D$ ( $\delta_2$ )	-0.2622	-0.2215	-0.2150	-0.2153	-0.2150
	${}^3S$ - ${}^3D$ ( $\varepsilon_1$ )	0.1104	0.0730	0.0583	0.0584	0.0583
104	${}^1S$ ( $\delta_0$ )	1.4652	-0.9166	0.0515	0.0796	0.0804
	${}^1P$ ( $\delta_1$ )	-0.5148	-0.4496	-0.4532	-0.4563	-0.4567
	${}^1D$ ( $\delta_2$ )	0.3628	0.1181	0.1241	0.1249	0.1249
	${}^3S$ - ${}^3D$ ( $\delta_0$ )	0.2415	0.2417	0.2962	0.2990	0.2990
	${}^3S$ - ${}^3D$ ( $\delta_2$ )	-0.3431	-0.3700	-0.3406	-0.3412	-0.3413
	${}^3S$ - ${}^3D$ ( $\varepsilon_1$ )	0.0133	0.1296	0.1005	0.1017	0.1018
176	${}^1S$ ( $\delta_0$ )	1.0134	-0.0234	-0.2099	-0.2161	-0.2162
	${}^1P$ ( $\delta_1$ )	-1.4466	-0.6896	-0.7077	-0.7087	-0.7079
	${}^1D$ ( $\delta_2$ )	1.4872	0.1595	0.1677	0.1651	0.1647
	${}^3S$ - ${}^3D$ ( $\delta_0$ )	0.2083	-0.1151	-0.0465	-0.0437	-0.0437
	${}^3S$ - ${}^3D$ ( $\delta_2$ )	-0.3717	-0.4815	-0.4390	-0.4344	-0.4338
	${}^3S$ - ${}^3D$ ( $\varepsilon_1$ )	-0.0939	0.1723	0.1481	0.1492	0.1494

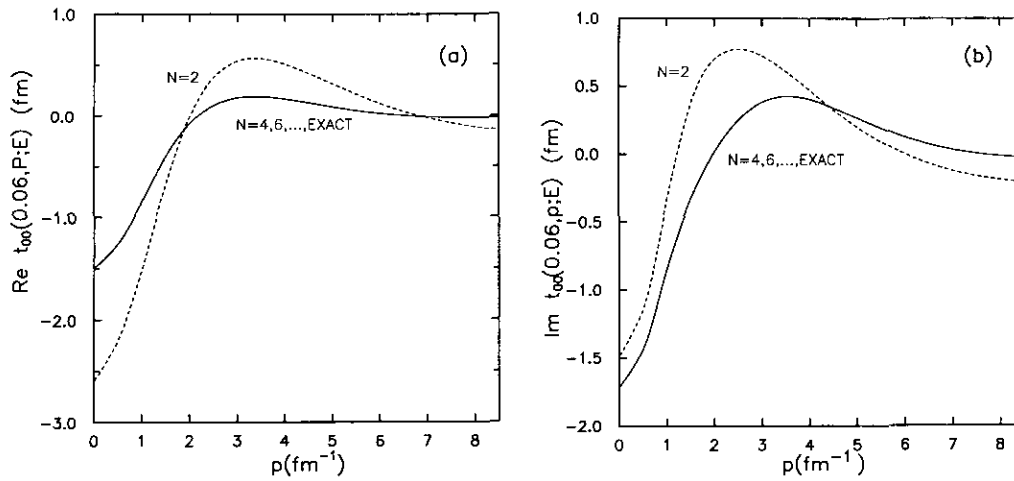


FIG. 1. The (a) real and the (b) imaginary parts of the off-shell  $t$  matrix elements  $t_{00}$  ( $0.06 \text{ fm}^{-1}$ ,  $p$ ; 48 MeV) versus  $p$  for various  $\mathcal{N}$ . The full line denotes the converged result.

as by direct matrix inversion or by iteration whenever available [4, 5, 8, 16, 17, 20]. The agreement between these results and the present results assured us of the absence of such errors.

The coupled  ${}^3S_1$ - ${}^3D_1$  channel is very interesting and deserves special attention because of the presence of the deuteron in this channel. It is interesting to exhibit the convergence in this channel diagrammatically for small  $\mathcal{N}$ . In Fig. 1 we plot the real and imaginary parts of the off-shell  $t$  matrix  $t_{00}$  ( $0.6 \text{ fm}^{-1}$ ,  $p$ ; 48 MeV) versus  $p$  for various  $\mathcal{N}$ . In Fig. 2 we plot the real and imaginary parts of the off-shell  $t$  matrix  $t_{22}$  ( $1.46 \text{ fm}^{-1}$ ,  $p$ ; 100 MeV) versus  $p$  for various  $\mathcal{N}$ . The convergence is good in both cases. We find in all cases that for small  $\mathcal{N}$  the convergence is

smooth and rapid. It is better than the convergence obtained previously with separable expansions or degenerate kernel method for the SRSC potential [8, 17] or similar realistic potentials for this channel.

In straightforward applications of Fredholm theory to the numerical solution of the Lippmann-Schwinger equation, the integral equation is basically transformed into a matrix equation which is then solved by matrix inversion, iteration, or otherwise. The infinite integral in this equation in momentum space is usually transformed into a discrete sum. In order to achieve a precision comparable to that of the present method one requires about 100 momentum mesh points [21]. That procedure in-

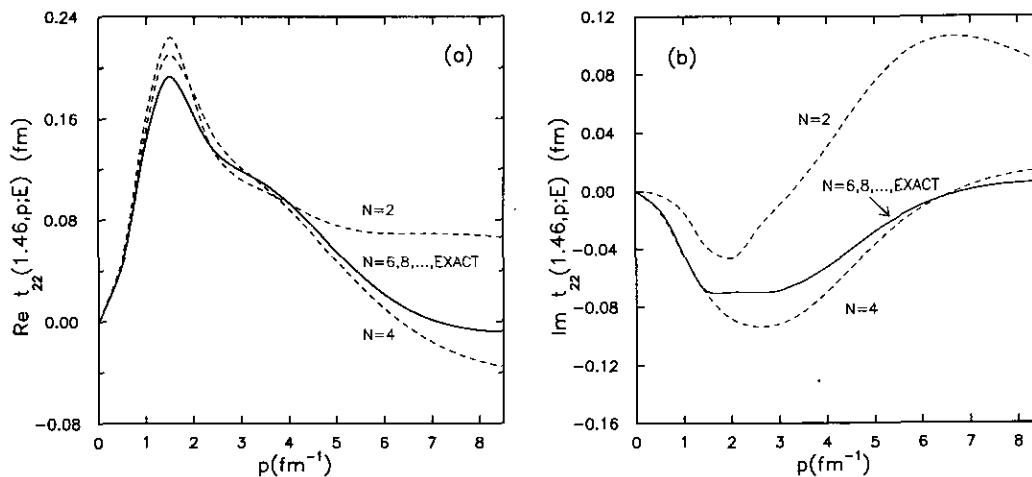


FIG. 2. The (a) real and the (b) imaginary parts of the off-shell  $t$  matrix  $t_{22}$  ( $1.46 \text{ fm}^{-1}$ ,  $p$ ; 100 MeV) versus  $p$  for various  $\mathcal{N}$ . The full line denotes the converged result.

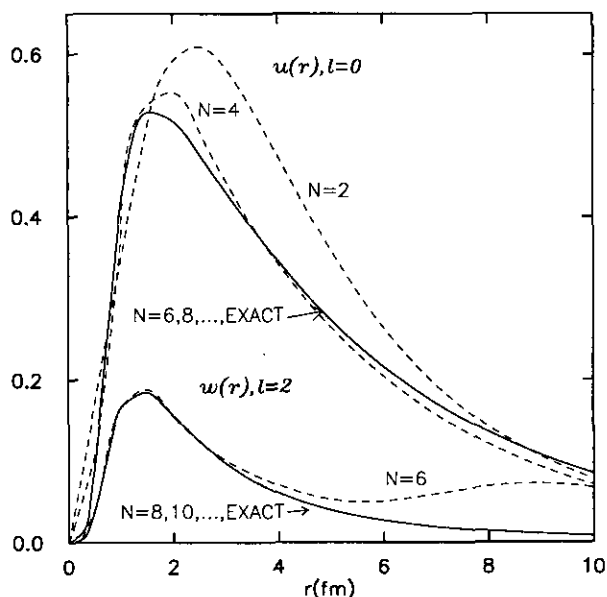


FIG. 3. The deuteron wave-functions  $u(r)$  (for  $L = 0$ ) and  $w(r)$  (for  $L = 2$ ) versus  $r$  for various  $N$ . The full line denotes the converged result.

volves handling  $100 \times 100$  matrices in momentum space. Similar precision is achieved in the present method via matrices of much smaller dimension.

Finally, we use the present method for calculating the deuteron bound state with the SRSC  ${}^3S_1$ - ${}^3D_1$  potential [17]. From the vanishing of the determinant of the matrix  $J^{-1}$  we found the binding energy in the  ${}^3S_1$ - ${}^3D_1$  channel to be 2.2298 MeV. We also calculated the asymptotic  $D$  state to  $S$  state ratio for the deuteron wave function defined by

$$\eta_d = \lim_{k \rightarrow i\beta} \frac{t_{02}}{t_{00}}. \quad (4.2)$$

We found the converged result for  $\eta_d$  for  $N > 8$  to be 0.02634. These values agree with the exact calculation of the deuteron bound state for this potential [17]. In Fig. 3 we exhibit the configuration space deuteron wave-functions  $u(r)$  (for  $L = 0$ ) and  $w(r)$  (for  $L = 2$ ) versus  $r$  for various  $N$ . The convergence of the wave-function is good in both cases. The function  $u(r)$  converges to the exact result for  $N = 6$ , and the function  $w(r)$  converges to the exact result for  $N = 8$ .

## V. SUMMARY

We have applied for the first time the complex Kohn v.p. for the solution of the LS equation for nucleon-nucleon scatter-

ing and the deuteron bound-state problem with the Reid soft-core potentials in several angular momentum channels, including the  ${}^3S_1$ - ${}^3D_1$  channel. We calculated the scattering phase-shifts, off-shell  $t$  matrix elements, the deuteron wave functions, and the deuteron  $D$  state to  $S$  state ratio. In all cases the convergence was very good and better than that obtained with the Schwinger v.p. for the same problem. This shows that the complex Kohn v.p. should be an efficient method for solving other few-nucleon problems including the trinucleon problem.

The work is supported in part by the Conselho Nacional de Desenvolvimento Científico e Tecnológico (CNPq) of Brasil.

## REFERENCES

1. J. Schwinger, *Phys. Rev.* **72**, 742 (1947); Lecture Notes, Harvard University, 1947 (unpublished).
2. W. Kohn, *Phys. Rev.* **74**, 1763 (1948); L. Hulthen, *K. Fysiogr Saelisk. Lund. Foern.* **14**, 257 (1944); *Ark. Mat. Astron. Fys. A*, **35**, No. 25 (1948).
3. For reviews on variational principles, see J. Callaway, *Phys. Rep.* **45**, 89 (1978); M. A. Abdel-Rauof, *Phys. Rep.* **84**, 163 (1982); **108**, 1 (1984); R. R. Lucchese, K. Takatsuka, and V. McKoy, *Phys. Rep.* **131**, 147 (1986); E. Gerjuoy, A. R. P. Rau, and L. Spruch, *Rev. Mod. Phys.* **55**, 725 (1983); R. K. Nesbet, *Adv. At. Mol. Phys.* **13**, 315 (1979).
4. S. K. Adhikari and K. L. Kowalski, *Dynamical Collision Theory and its Applications* (Academic Press, Boston, 1991).
5. S. K. Adhikari and I. H. Sloan, *Phys. Rev. C* **11**, 1133 (1975); S. K. Adhikari and L. Tomio, *Phys. Rev. C* **36**, 1275 (1987).
6. I. H. Sloan and T. J. Brady, *Phys. Rev. C* **6**, 701 (1972).
7. K. Takatsuka, R. R. Lucchese, and V. McKoy, *Phys. Rev. A* **24**, 1812 (1981); K. Takatsuka and V. McKoy, *Phys. Rev. A* **23**, 2352 (1981).
8. S. K. Adhikari and I. H. Sloan, *Nucl. Phys. A* **251**, 297 (1975).
9. B. A. Lippmann and J. Schwinger, *Phys. Rev.* **79**, 469 (1950).
10. C. Schwartz, *Phys. Rev.* **124**, 1468 (1961).
11. W. H. Miller and B. M. D. D. Jansen op de Haar, *J. Chem. Phys.* **86**, 6213 (1987).
12. Y. Mito and M. Kamimura, *Prog. Theor. Phys.* **56**, 583 (1976); J. Z. H. Zhang, S.-I. Chu, and W. H. Miller, *Prog. Theor. Phys.* **88**, 6233 (1988); T. N. Rescigno and B. I. Schneider, *Phys. Rev. A* **36**, 2061 (1987); B. I. Schneider and T. N. Rescigno, *Phys. Rev. A* **37**, 3749 (1988).
13. R. R. Lucchese, *Phys. Rev. A* **40**, 6879 (1989); S. K. Adhikari, *Chem. Phys. Lett.* **189**, 340 (1992).
14. L. F. X. Gaucher and W. H. Miller, *Israel J. Chem.* **29**, 349 (1989).
15. W. H. Miller, *Ann. Rev. Phys. Chem.* **41**, 245 (1990); D. G. Truhlar et al., *J. Chem. Phys.* **99**, 2739 (1993).
16. R. V. Reid, *Ann. Phys. (N. Y.)* **50**, 411 (1968).
17. S. Peiper, *Phys. Rev. C* **9**, 883 (1974).
18. H. P. Stapp, T. Ypsilantis, and N. Metropolis, *Phys. Rev.* **105**, 302 (1957).
19. J. M. Blatt and L. C. Biedenharn, *Phys. Rev.* **86**, 399 (1952).
20. J. Haidenbauer and W. Plessas, *Phys. Rev. C* **27**, 63 (1983); G. H. Rawitscher and G. Delic, *Phys. Rev. C* **29**, 747 (1984); G. H. Rawitscher, *Phys. Rev. C* **25**, 2196 (1982); K. Hartt and P. V. A. Yidana, *Phys. Rev. C* **36**, 475 (1987); E. F. Redish and K. Stricker-Bauer, *Phys. Rev. C* **36**, 513 (1987).
21. J. Horacek and T. Sasakawa, *Phys. Rev. C* **32**, 70 (1985).